

See discussions, stats, and author profiles for this publication at: <https://www.researchgate.net/publication/325474521>

Design of a thermoelectric generator for electrical active implants

Conference Paper · October 2017

CITATIONS

2

READS

45

1 author:



[Onkar Sandip Jadhav](#)

Technische Universität Berlin

4 PUBLICATIONS 4 CITATIONS

SEE PROFILE

Some of the authors of this publication are also working on these related projects:



Model order reduction for parametric high dimensional models in the analysis of financial Risk [View project](#)

Entwurf eines thermoelektrischen Generators für elektrisch aktive Implantate

Design of a thermoelectric generator for electrical active implants

B.Sc. Onkar Sandip Jadhav², M.Sc. Cheng Dong Yuan^{1,2}, Prof. Dr.-Ing. Dennis Hohlfeld², Prof. Dr.-Ing. Tamara Bechtold^{1,2}

¹Department of Engineering, Jade University of Applied Sciences, Wilhelmshaven, Germany

²Institute of Electronic Appliances and Circuits, University of Rostock, Rostock, Germany

Kurzfassung

Elektrisch aktive Implantate für regenerative Therapien (z.B. Regeneration von Knochen sowie tiefe Hirnstimulation zur Behandlung von Bewegungsstörungen) gewinnen in einer alternden Population zunehmend an Bedeutung. Die Implantate müssen im Verlauf der Therapie ausgetauscht werden. Ihre Leistungsanforderungen variieren von wenigen Mikrowatt bis zu einigen Milliwatt und werden mit zunehmendem Funktionsumfang weiter steigen. Um die Lebensdauer elektrisch aktiver Implantate zu verlängern und damit die aufwendige und riskante Operation zum Tausch des Implantats verzichtbar zu machen, soll ein erheblicher Teil seines Energiebedarfs durch die Wandlung mechanischer oder thermischer Körperenergie in elektrische Leistung gedeckt werden. In dieser Arbeit stellen wir ein multiphysikalisches Modell eines miniaturisierten thermoelektrischen Generators für elektrisch aktive Implantate vor, welcher den Temperaturgradienten im menschlichen Gewebe nutzt. Wir analysieren anhand eines Modells den Einfluss der Geometrie- und Materialparameter auf die thermischen und elektrischen Eigenschaften und leiten Aussagen über einen optimierten Wandlerentwurf ab. Weiterhin, setzen wir die mathematischen Methoden der Modellordnungsreduktion ein, um ein genaues kompaktes Modell zu erzeugen, das im Rahmen einer System Simulation eingesetzt werden kann.

Abstract

Electrically active implants for regenerative therapies (e.g. regeneration of bone tissue or deep brain stimulation for the treatment of motion disorders) are gaining on importance within an aging population. The implants must be replaced during the course of the therapy. Their performance requirements vary from a few microwatts to a few milliwatts and will keep increasing with growing functionality. In order to extend the life of electrical active implants and thus avoid the expensive and risky operations for their replacement, a considerable amount of the implant's energy requirement shall be covered by the conversion of mechanical or thermal body energy into electrical power. In this work, we present a multiphysical model of a miniaturized thermoelectric generator for electrically active implants, which uses temperature gradients in human tissue. Based on this model, we analyze the influence of the geometry and material parameters on the thermal and electrical properties and aim for an optimal transducer design. Furthermore, we use mathematical methods of model order reduction to create an accurate compact model that can be applied within a system simulation.

1 Introduction

European populations are ageing rapidly. By the year 2060, every third person living in Germany will be older than 65 years. For this reason, the social and socio-economic relevance of regenerative therapies is clearly increasing. This holds particularly true for implants: the older the population grows, the more medical implants for various indication areas are required and the more often they have to be replaced during the course of therapy. The research vision pursued by the CRC 1270 ELAINE (ELectrically Active ImplaNts) focuses on novel electrical active implants. In particular, ELAINE addresses implants employed for the regeneration of bone and cartilage, and implants for deep brain stimulation to treat movement disorders. Its first objective is to establish innovative energy autonomous implants that allow a feedback-controlled electrical stimulation.

To improve an implant's lifetime, it is a reasonable endeavor to satisfy a significant share of its energy demand

by means of harvesting mechanical or thermal ambient energy. Thermoelectric techniques (utilizing the Seebeck effect) with microstructured energy converters have been explored for application on the skin's surface [1]-[3] for powering pulse oximetry and electroencephalography sensors. If a temperature difference is established across such a device, a Seebeck voltage is generated, which is directly proportional to the temperature difference.

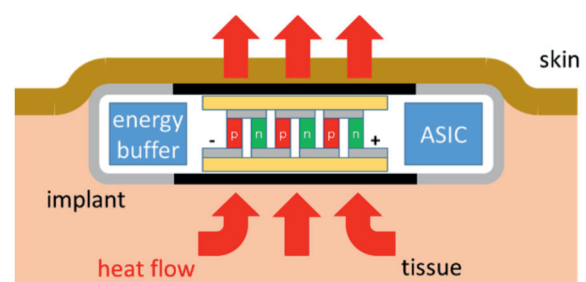


Figure 1 Schematics of a thermo-electrically driven implant for application below the skin.

In this work we present a new design of thermoelectric power generator (TEG) for electrically active implants. It is based on the power dissipation of the human body, with the heat leaving the body by heat convection through the skin. The envisioned design is shown schematically in **Figure 1**. The voltage generated by a TEG is also directly proportional to the number of leg pairs.

In the following we present a multi-physical finite-element-based model of a miniaturized TEG and analyze the influence of the geometry on the thermal and electrical properties. Furthermore, we apply mathematical model order reduction (MOR) in order to come up with a compact but highly accurate thermal model, which can be employed for a time-transient co-simulation with a power management circuitry.

2 Case Study

We use a simplified tissue model consisting of muscle, fat and skin layers [3]. The heat conduction in the tissue is described by the bioheat equation of Pennes [4], which considers the perfusion (blood circulation) as an additional heat source:

$$\kappa \nabla T(\vec{r}) + Q_b + Q_m = 0 \quad (1)$$

with $Q_b = \rho_b c_b \omega_b (T_a - T(\vec{r}))$ and Q_m as metabolic heat generation rate. Where ρ , c , κ are the density, specific heat capacity and thermal conductivity of the tissue types, ρ_b , c_b describe the thermal properties of blood, and ω_b is a measure of perfusion. $T(\vec{r})$ is the resulting temperature distribution and T_a is the temperature of the arterial blood, which is assumed constant with $T_a = 37^\circ\text{C}$. Furthermore, a constant body core temperature of 37°C is assumed. The heat is dissipated by convection at the skin surface with a heat transfer coefficient of $h = 20 \text{ W}/(\text{m}^2 \text{ K})$ whereas the environmental temperature is set to 14.85°C . Used material properties are specified in Table 1.

	muscle	fat	skin
thickness [mm]	71	4,0	5,0
density ρ [kg/m ³]	1000	1000	1000
specific heat c [J/(kg K)]	4200	4200	4200
therm. conductivity κ [W/(m K)]	0,5	0,2	0,3
metabolic heat Q_m [W/m ³]	420	0	0
perfusion rate ω_b [ml/(s g)]	$5 \cdot 10^{-4}$	0	0

Table 1: Material parameters of the thermal tissue model, adopted from [5].

Figure 2 shows the resulting temperature profile through the tissue. The temperature gradient is the highest within the fat layer, due to its low thermal conductivity.

The voltage generated by a TEG is given by

$$V_{out} = n \cdot \Delta T (\alpha_1 - \alpha_2) \quad (2)$$

where ΔT is the temperature difference, n is the number of thermocouples, and $\alpha_{1,2}$ are the Seebeck coefficients of the thermocouple legs. In this work, we model a TEG with 81

legs (see **Figure 3**) of bismuth telluride ($\kappa_{th} = 1,35 \text{ W}/\text{m}\cdot\text{K}$, $\alpha = \pm 200 \mu\text{V}/\text{K}$, $\rho_{el} = 10 \mu\Omega \text{ m}$). The TEG has a foot print of $9 \times 9 \text{ mm}^2$ and is integrated into a cylindrical housing (diameter 15 mm, height 3 mm) which is made of a polymer of low thermal conductivity ($\kappa_{th} = 0,25 \text{ W}/\text{m}\cdot\text{K}$) and metallic top and bottom sides for optimal thermal contact to the body tissue. The embedding of the TEG into the fat layer utilizes a high temperature difference. The series electrical connection of all elements delivers the output voltage of the TEG.

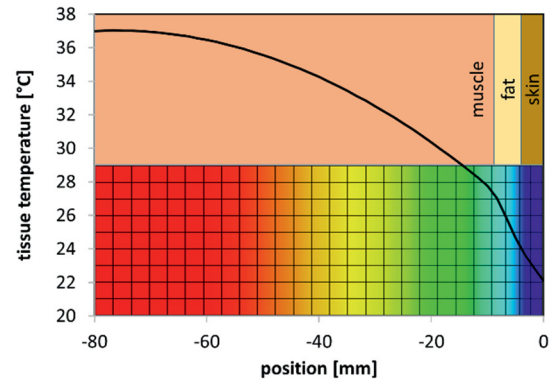


Figure 2 Temperature profile inside human body tissue (no implant / TEG present). Perfusion and metabolic heat in the muscle act as heat sources. Highest change in temperature can be observed across the fat layer.

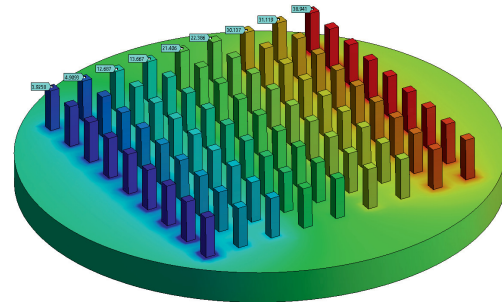


Figure 3 Configuration of the thermocouples (81 legs in total, top plate not shown). The color gradient indicates the evolution of the thermoelectric voltage generation, computed within finite element simulation. The series connection of the p- and n-type legs results in an output voltage of 80 mV at a temperature difference of 2,48 K.

3 Design Optimization

Choosing the right geometry for the thermoelectric generator poses an optimization problem. If the cross section of the thermocouple legs is increased, the generator's electrical resistance decreases and thus the electrical power output improves (as long as the temperature difference and hence, the output voltage is kept constant). However, the thermal resistance decreases as well, which causes a drop in temperature difference across the TEG and consequently leads to a smaller voltage output. One needs to balance these opposite effects in order to find an optimum leg size. We thus analyzed the impact of the leg's cross section on

the thermal properties and electrical performance of the TEG.

Figure 4 shows that the open circuit voltage of the TEG decreases with the increasing cross-section of the leg. The electrical power delivered in a matched load resistor reaches a maximum of 94,5 μW at a cross-section of 275 \times 275 μm^2 .

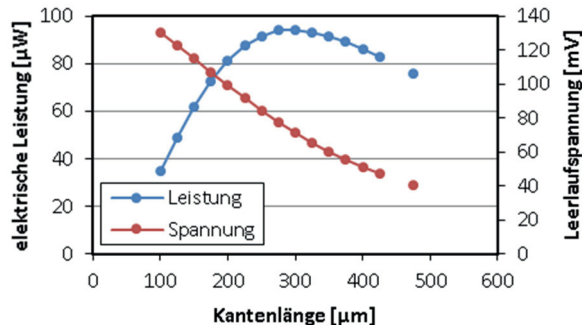


Figure 4 Maximum electrical power is obtained for a leg edge length of 275 μm , smaller dimensions cause an excessive electrical resistance; wider legs will lead to a drop in temperature difference.

The finite element analysis of the temperature field across the tissue shows that the presence of the TEG has only a minor impact on the temperature field itself. This indicates a good thermal match between the TEG housing and the surrounding tissue. In the following a compact thermal model is constructed and employed within a system level simulation.

4 Compact Thermal Model

After the spatial discretization with the finite element method, the thermal transient model can be represented as:

$$\sum_n \begin{cases} E \cdot \dot{T}(t) = A \cdot T(t) + B \cdot u \\ y(t) = C \cdot T(t) \end{cases} \quad (3)$$

where, $A, E \in \mathbb{R}^{n \times n}$ are the global heat conductivity and heat capacity matrices, $B \in \mathbb{R}^{n \times m}$ is the input matrix and $C \in \mathbb{R}^{n \times p}$ is the output matrix. Here, $n = 106467$ is the dimension of the system and m and p are the number of inputs and user defined outputs, respectively. We have a single heat generation input and three different temperature outputs: one at the skin surface and two at the top and bottom of the TEG. For the purpose of performing model order reduction, we assume a homogenous heat generation rate of 2200 W/m^3 within the muscle layer. Dirichlet and convection boundary conditions are specified in section 2. In this work, a mathematical Krylov subspace-based model order reduction is applied, which has already been proven to work well for linear thermal models [6]. A basic idea of mathematical MOR is to project the original high-dimensional state-vector $T(t)$ onto some lower-dimensional subspace $V \in \mathbb{R}^{n \times r}$ as follows:

$$T(t) = V \cdot z(t) + \varepsilon \quad (4)$$

The goal is to find V , such that the projection error ε can be neglected. When the subspace is found, equation (3) is

projected by applying (4) and then multiplying (3) from the left side by V^T :

$$\sum_r \begin{cases} E_r \cdot \dot{z}(t) = A_r \cdot z(t) + B_r \cdot u \\ y(t) = C_r \cdot z(t) \end{cases} \quad (5)$$

where $E_r = V^T E V$, $A_r = V^T A V$, $B_r = V^T B$, $C_r = C V$. The reduced system (5) is of the same form as (3), but with much smaller dimension $r \ll n$. In Krylov subspace-based MOR, V is usually constructed as an orthonormal basis of the right Krylov-subspace, defined as follows:

$$K_r\{P, b\} = \text{span}\{b, P^2 b, \dots, P^{r-1} b\} \quad (6)$$

For reducing (3) we set $P = A^{-1}E$ and $b = A^{-1}B$. For constructing V , we use the Block-Arnoldi algorithm from [7] as implemented in MOR inside ANSYS [8].

For transient simulation, the film coefficient was changed to 15 $\text{W}/(\text{m}^2 \text{K})$ to represent typical daily human body activity. A steady state temperature distribution, obtained with a film coefficient of 20 $\text{W}/(\text{m}^2 \text{K})$, was considered as an initial state. **Figure 5** shows an excellent match between the temperature distribution of the full scale model of order 106.467 and the reduced order the model of order 30. The computational time of the reduced model is several orders of magnitude shorter than that of the full model (see **Table 2**).

System size	Full model (106467 DOF)	Reduced model (30 DOF)
Computational time (seconds)	1205	12.8

Table 2: Comparison of the computational time of full and reduced models (Intel Xeon E5-2680, 2.5 GHz, 128 GB RAM, 4 active cores).

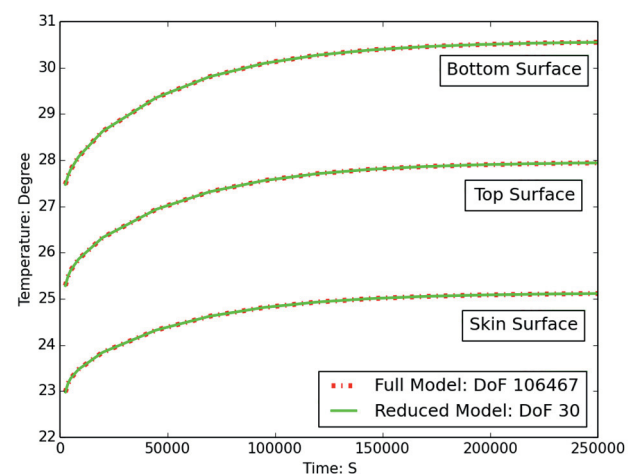


Figure 5 Temperature result comparison between full and reduced model at top surface, bottom surface and skin surface of the TEG model.

The reduced order model will be applied within the device-circuit co-simulation.

5 System Level Simulation

The reduced system (5) can be transformed into the state-space form, as schematically represented in **Figure 6** and imported into the system level simulator *ANSYS Simplorer* for co-simulation with electrical circuitry.

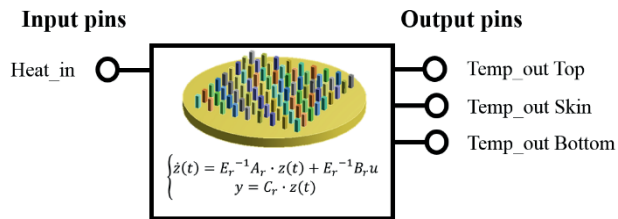


Figure 6 Reduced TEG model in the state-space form.

Figure 7 shows a simple co-simulation setup. The temperature difference $\Delta T = 2.6^\circ\text{C}$ is obtained by subtracting top and bottom output temperatures. The voltage output is given by (2). This voltage has been implemented in the system level model as a controlled voltage source. Furthermore, R_1 models the internal resistance of the TEG, while R_2 is the resistive load (representing e.g. the input impedance of a DC/DC boost converter). For impedance matching we vary it from 1Ω to 100Ω , as shown in **Figure 8**.

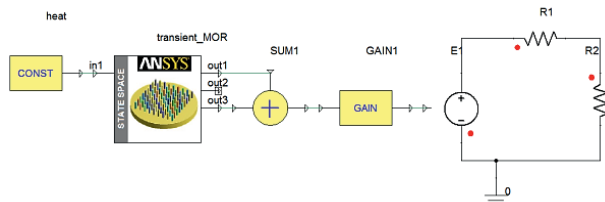


Figure 7 Co-simulation setup with state space model of transient thermal analysis to evaluate power output.

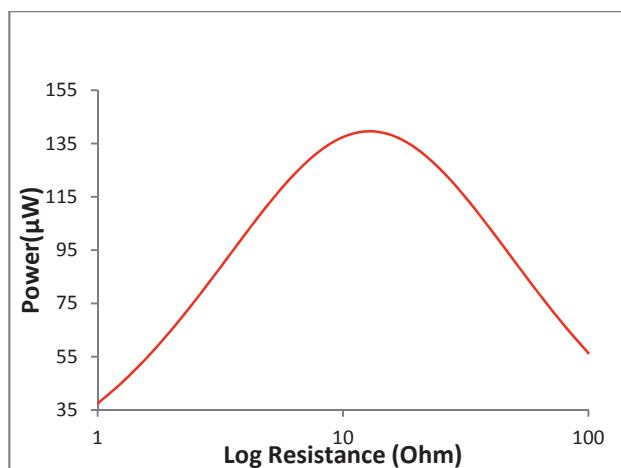


Figure 8 Power dissipated in load resistance for different load resistance values.

The calculated voltage is 84,72 mV. This level can be converted to a higher voltage suitable to drive the circuitry of implants.

6 Conclusion and Outlook

By means of a thermo-electrical model we studied the impact of the thermocouple leg's cross section on electrical power output. It was further shown that an optimum dimension exists for which power is maximized.

Transient thermal simulation was performed to evaluate the effect of a change in the convection boundary condition. Mathematical model order reduction was applied to enable the device-circuit co-simulation. Further improvement will be to construct a parametric reduced order model with the heat transfer coefficient as an additional input and to take into account the temperature-dependence of blood perfusion during model order reduction.

7 References

- [1] M. Koplow, A. Chen, D. Steingart, P. K. Wright, and J. W. Evans. Thick film thermoelectric energy harvesting systems for biomedical applications, in 5th International Summer School and Symposium Medical Devices and Biosensors, 2008, pp. 322–325.
- [2] C. Watkins, B. Shen, and R. Venkatasubramanian, Low-grade-heat energy harvesting using superlattice thermoelectrics for applications in implantable medical devices and sensors” in 24th International Conference on Thermoelectrics, 2005, pp. 265–267.
- [3] Y. Yang, X.-J. Wei, and J. Liu, Suitability of a thermoelectric power generator for implantable medical electronic devices, in Journal of Physics D: Applied Physics 40(18), pp. 5790–5800.
- [4] H. H. Pennes, Analysis of tissue and arterial blood temperatures in the resting human forearm, in Journal of applied physiology, 1(2), pp. 93-122.
- [5] Z. S. Deng and J. Liu, Mathematical modeling of temperature mapping over skin surface and its implementation in thermal disease diagnostics, in Computers in Biology and Medicine. 34(6), pp. 495-521.
- [6] T. Bechtold, E. B. Rudnyi, J. G. Korvink, “Fast Simulation of Electro-Thermal MEMS: Efficient Dynamic Compact Models”, Springer Verlag, Heidelberg, Series: MEMS and Microtechnology, (ISBN 978-3-540-34612-8), (2006).
- [7] R. W. Freund, (2000): ‘Krylov-subspace methods for reduced-order modeling in circuit simulation’. Journal of Computational and Applied Mathematics, p. 395-421.
- [8] E. B. Rudnyi, MOR for ANSYS. In: System-level modeling of MEMS, Wiley VCH book series on advanced micro and nanosystems, p. 425438, (2003)